NOTES AND CORRESPONDENCE

Regional Climate Model Projections and Uncertainties of U.S. Summer Heat Waves

KENNETH E. KUNKEL

Division of Atmospheric Sciences, Desert Research Institute, Reno, Nevada, and Illinois State Water Survey, University of Illinois at Urbana–Champaign, Champaign, Illinois

XIN-ZHONG LIANG AND JINHONG ZHU

Illinois State Water Survey, University of Illinois at Urbana–Champaign, Champaign, Illinois

(Manuscript received 16 July 2009, in final form 26 March 2010)

ABSTRACT

Regional climate model (RCM) simulations, driven by low and high climate-sensitivity coupled general circulation models (CGCMs) under various future emissions scenarios, were compared to projected changes in heat wave characteristics. The RCM downscaling reduces the CGCM biases in heat wave threshold temperature by a factor of 2, suggesting a higher credibility in the future projections. All of the RCM simulations suggest that there is a high probability of heat waves of unprecedented severity by the end of the twenty-first century if a high emissions path is followed. In particular, the annual 3-day heat wave temperature increases generally by 3°–8°C; the number of heat wave days increases by 30–60 day yr^{-1} over much of the western and southern United States with slightly smaller increases elsewhere; the variance spectra for intermediate, 3–7 days (prolonged, 7–14 days), temperature extremes increase (decrease) in the central (western) United States. If a lower emissions path is followed, then the outcomes range from quite small changes to substantial increases. In all cases, the mean temperature climatological shift is the dominant change in heat wave characteristics, suggesting that adaptation and acclimatization could reduce effects.

1. Introduction

Heat waves can have notable adverse effects on human health during the summer season in the United States. For example, heat waves in 1995 and 1999 resulted in 739 and 110 excess deaths, respectively, in Chicago, Illinois, alone (Whitman et al. 1997; Palecki et al. 2001). During such events, residents in urban centers may be particularly at risk because of such factors as elevated temperatures from the urban heat island effect, poverty, a generally older population often living alone, and reduced home ventilation because of the fear of crime (Changnon et al. 1996). In addition to the direct effects of heat, urban air quality can also be adversely affected because of the temperature dependence of relevant chemical reactions, causing secondary effects on health. The projections of warmer conditions arising from anthropogenic forcing of the climate system lead to an expectation of more frequent and/or intense heat waves with associated increased risks of adverse health consequences. The purpose of this study is to quantify the potential future changes in heat waves as well as the associated uncertainties, using a well-developed regional climate model and focusing on urban areas, particularly two large population centers (Chicago and the Northeast urban corridor) that are vulnerable to excessive heat.

In a past study, output from the National Center for Atmospheric Research–U.S. Department of Energy Parallel Climate Model (PCM) for 2080–99, using two measures of extreme heat, indicated that heat waves will increase in intensity, frequency, and duration (Meehl and Tebaldi 2004). In that model simulation, which assumed a business-as-usual emissions scenario, the temperature of the worst 3-day heat wave generally increased by 2°–3°C over the United States, with the largest increases found in the West and South. There is a considerable range in the climate sensitivity of coupled atmosphere–ocean general circulation models (CGCMs), and it is

Corresponding author address: Kenneth E. Kunkel, Desert Research Institute, 2215 Raggio Parkway, Reno, NV 89512.
E-mail: kenneth.kunkel@dri.edu

DOI: 10.1175/2010JCLI3349.1

© 2010 American Meteorological Society

logical to expect that the projections of the frequencies and intensities of extremes will also vary by a sizeable amount. Thus, the results from a single model are very useful at establishing the potential for changes of societal and/or environmental significance, but they do not provide information about the possible range of future conditions. Such information is needed by those in decision-making capacities to evaluate options for mitigation and adaptation. An analysis of simulations from multiple models with differing climate sensitivities and emissions scenarios provides insights into the uncertainties of future conditions.

The spatial resolution in the typical modern CGCM is too coarse to adequately simulate some processes important to regional climate features, often leading to biases in the mean climate. Regional climate models (RCMs) have the potential to reduce biases through higher spatial resolution, with a typical grid spacing of a factor of 5–10 smaller than most CGCMs, and more complete representation of physical processes. A RCM downscaling of PCM projections was found to produce a more realistic present-day climate and subsequently a different future climate projection than the driving PCM itself (Liang et al. 2006). The differences were particularly notable in the central United States and appeared to arise from a more complete physical representation, including convection parameterization in the RCM. Recently, a RCM downscaling analysis (Liang et al. 2008) demonstrated that major biases in CGCM simulations of the present-day climate appear to be systematically propagated into future climate projections at regional scales; for example, in the PCM a nonrealistic summer precipitation peak in Colorado in the present-day control simulation also appears as a peak in the future simulation. They showed that a nested RCM–GCM approach substantially reduces the biases in representing the present climate and also likely provides higher skill in downscaling the future climate projection. For the reasons mentioned earlier, the present study uses the RCM downscaling approach to investigate the likely outcome and uncertainty of future projections of heat waves.

2. Methods

Like CGCMs, RCMs require large computer resources; therefore, it is imperative to carefully select experiments to adequately sample both the different CGCM climate sensitivities and future emissions paths. To this end, the RCM simulations were driven by two CGCMs: (i) the PCM (Washington et al. 2000), a low climate-sensitivity model; and (ii) the Hadley Centre Atmospheric GCM 3P (HadAM3P) derived from the atmospheric GCM (Pope et al. 2000) of the third climate configuration of the Met Office Unified Model (HadCM3; Johns et al. 2003), a higher climate-sensitivity model (Kunkel and Liang 2005). The HadAM3P was run with observed SSTs for the present-day climate. For HadAM3P's future climate simulation, monthly-mean changes in SSTs between the present-day (1961–90) and future (2071–2100) were obtained from simulations of HadCM3. These changes were added to time series of observed present-day SSTs to drive HadAM3P (Rowell 2005); this procedure means that the interannual variability of SSTs is the same in present and future simulations. Such HadAM3P runs, considered as improved outcomes of the HadCM3 with finer resolution, have been widely used in climate change impact studies, such as the Prediction of Regional scenarios and Uncertainties for Defining European Climate Change Risks and Effects (PRUDENCE) project (Christensen et al. 2002).

Two PCM simulations were available for the Intergovernmental Panel on Climate Change Special Report on Emissions Scenarios (Nakicenovic et al. 2000), the A1Fi (high, effective CO_2 concentration of ~970 ppm by 2100) and B1 (low, ~550 ppm by 2100) emissions scenarios. The required 6-h resolution data for one control (1991–2000) and one future (2090–2099) period were available. Two HadAM3P simulations were also available for the A2 (moderately high, ~860 ppm by 2100) and B2 (moderately low, ~620 ppm by 2100) emissions scenarios. Note that the two emissions scenarios used in the HadAM3P (hereafter "HAD") simulations are intermediate between the two extreme scenarios used in the PCM. Six-hour data were obtained for a control period (1980–89) and for one future period (2090–99). Although the two CGCM modeling centers did not have driving CGCM data for identical emissions scenarios at the RCM-required 6-h time resolution, thus precluding a direct model-to-model comparison of results, the available data nevertheless permit exploration of a large range of potential future projections from low emissions with a low climate-sensitivity model to moderately high emissions with a high climate-sensitivity model.

The RCM used in this study is a climate extension of the fifth-generation Pennsylvania State University–National Center for Atmospheric Research Mesoscale Model (Liang et al. 2004, 2006). The spatial resolution of the simulations is 30 km. Using the entire period of availability of CGCM data, the RCM simulations were 11 yr in length and were performed continuously starting on 1 January, with the initial year considered as a spinup and the last 10 yr as the analysis period. The PCM (HAD)-driven simulations are denoted as RCM-P (RCM-H).

Observational data were obtained from 7235 stations in the U.S. Cooperative Observer Program network.

This consisted of daily observations of maximum and minimum temperatures. These data were gridded onto the 30-km RCM grid. They are concurrent with the GCM present-climate simulation period, that is, 1991–2000 for PCM and 1980–89 for HAD. Observations showed small differences between the two periods (see later in paper), inconsistency of which does not affect our results. For longer-term analysis of variability, a subset of 807 stations was selected; these stations have less than 10% missing data over the period of 1895–2006.

Two measures of extreme heat were explored. One analysis examined the worst 3-day heat wave, as measured by the 3-day mean temperature, in each year of the entire 10-yr period; we term this the ''annual heat wave.'' A second analysis defined a heat wave using percentile-based thresholds of daily mean temperature by the same definition as Meehl and Tebaldi (2004) as follows. A period was considered a heat wave if the following criteria were met: (i) the daily mean temperature was above the 97.5 percentile threshold for at least 3 days during the period; (ii) the average daily mean temperature during the entire period exceeded the 97.5 percentile threshold; and (iii) the daily mean temperature exceeded the 81 percentile threshold for every day of the period. The percentile thresholds were based on data for May–September (Huth et al. 2000). The longest such period satisfying the three criteria was considered a single heat wave (even if subperiods also met the criteria). Once each heat wave was identified, the number, average duration, and the total number of heat wave days was calculated for each year. The percentile threshold temperatures from the control simulation were used to identify heat waves in both the control and future period simulations.

Any changes in heat wave frequency and intensity may be a reflection of more general changes in the statistical properties of daily temperature distributions. To explore more broadly such possible changes, other metrics were calculated. These included the lag autocorrelation and a spectral analysis of gridpoint time series of temperature using the fast Fourier transform. Spectral results were analyzed for two periods: 3–7 and 7–14 days. These periods were chosen to correspond to the lengths of some notable historical heat waves. For example, the Chicago heat wave of 1995 was a 4-day event, while the worst heat wave of the twentieth century in the upper Midwest, occurring in July 1936, lasted about 2 weeks during its most intense phase. The lag autocorrelation and spectra were computed separately for each summer of the simulation to focus on those characteristics during the heat wave season. Then they were averaged for all summers in each simulation.

In all cases, results for future projections are presented as the model's future value minus the model's control simulation value. This assumes that biases in the control simulation for a particular model are very similar, in that the model's future projection and differencing in this way will largely remove such biases.

The statistical significance of the differences between future and control simulations was evaluated using Student's two-sample t test. It was assumed that each year's heat wave characteristics were independent of other years and then each year represents a single sample. The heat wave metric values (annual 3-day heat wave magnitude, number of heat wave days, lag correlation coefficient) for each simulation year were averaged and a standard deviation was calculated. The t statistic was calculated as follows:

$$t = (H_f - H_c)/S_{fc}$$

$$S_{fc} = \sqrt{(S_f^2 + S_c^2)/2},$$

where H is the average value of heat wave metric, S is the standard deviation of heat wave metric, $n = 10$ is the number of simulation years, and subscripts f and c indicate future and control simulations, respectively. The two-tailed t-test probability (p) value was determined from standard tables, subsequently defining the statistical significance of the results.

The simulation results were examined in detail for two major urban centers where the mortality rate is sensitive to excessive heat (Kalkstein and Greene 1997): Chicago and the northeastern coastal United States, including Philadelphia, Pennsylvania; New York City, New York; and Boston, Massachusetts. These centers occasionally experience intense heat waves; however, the frequency is sporadic and the population does not typically acclimatize fully to the intensity, increasing human vulnerability. By contrast, the mortality rates of more southern urban areas exhibit little sensitivity to excessive heat, perhaps because urban housing is more suitable for hot weather (Kalkstein 1993) and the people are more acclimatized to hot weather. Grid boxes where the population density exceeds 400 km^{-2} were included in this urban analysis. The future simulation period is often abbreviated in the following text as 2090s for 2090–99.

3. Results

a. Comparison with observations

The control simulation values (Figs. 1c–f) of the 97.5 percentile threshold temperature were compared with observations (Figs. 1a,b). The PCM control simulation, which was compared with the observations for the 1990s

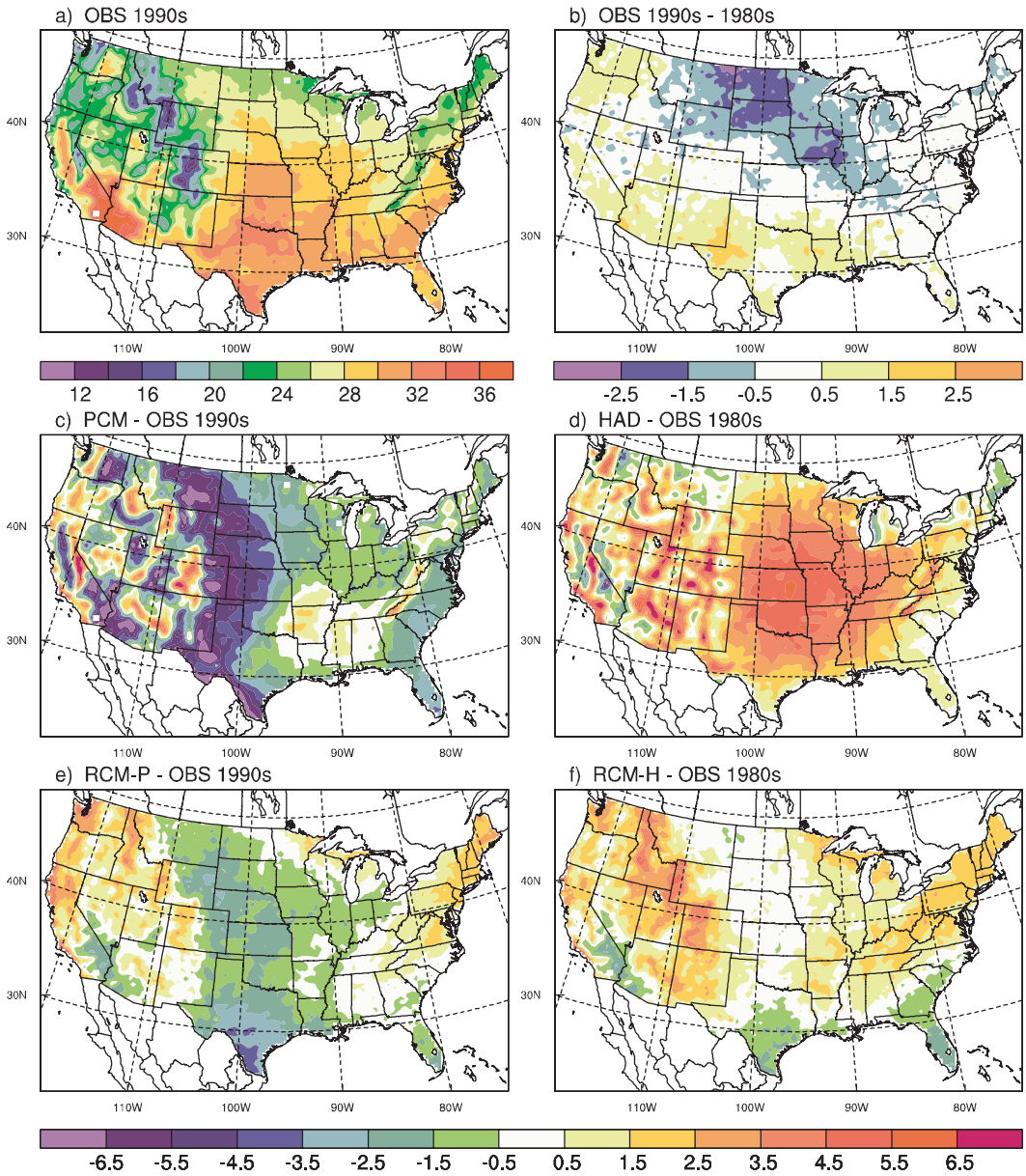

FIG. 1. Observed 97.5 percentile temperature threshold (°C) for the (a) 1990s and (b) differences between the 1980s and 1990s. Difference between model control simulations and observations for the 97.5 percentile summer temperature threshold for (c) PCM, (d) HAD, (e) RCM-P, and (f) RCM-H.

(Fig. 1a), produces large cold biases in the Great Plains just to the east of the Rocky Mountains of more than −6°C in some locations. The RCM-P generally produces smaller biases. This is particularly true in the Great Plains, where the biases are in the range of −1° to −3°C in the RCM-P compared to −6°C or more in the PCM. The domain-average absolute differences are 2.5°C for PCM and 1.2°C for RCM-P.

The observed values for the 1980s (Fig. 1b) are generally within 1.5°C of those for the 1990s (Fig. 1a). The HAD values are generally higher than the 1980s observed, particularly in the central United States, where warm biases exceed 5°C. The RCM-H reduces the HAD warm biases considerably, most notably in the central United States, where the HAD biases are largest. The average (over the U.S. domain) absolute differences between model control simulations and observations are 2.5°C for HAD and 1.2°C for RCM-H.

Although the signs of the major biases are opposite between HAD and PCM, the RCM produces values

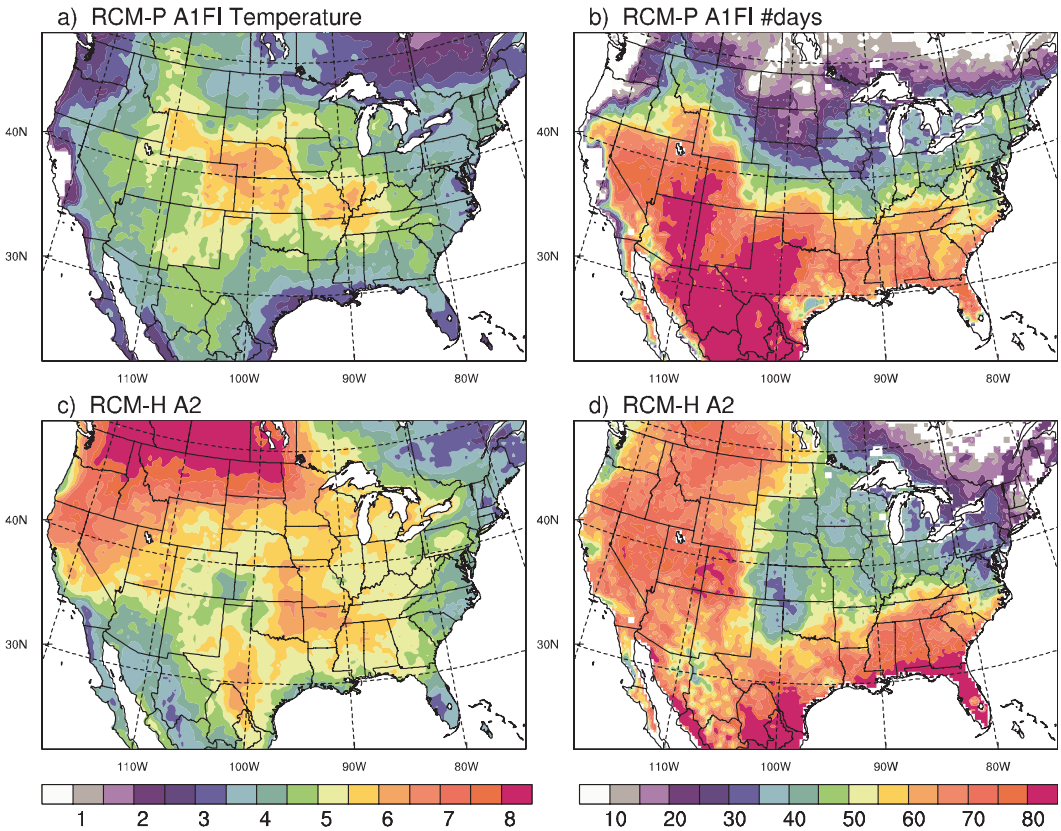

FIG. 2. Projections of change in the (a),(c) average annual 3-day heat wave temperature (°C) and (b),(d) average annual number of heat wave days. Simulations include the (a),(b) RCM-P A1Fi and (c),(d) RCM-H A2 emissions scenarios.

much closer to observed in both cases, reducing the overall average biases by a factor of 2. This suggests that the major biases of the CGCM control simulations are being produced in large part by processes internal to the RCM domain, not by large-scale circulation patterns near the lateral boundaries of the RCM domain. Thus, the more complete physics and higher resolution of the RCM are able to correct these biases.

The results for mean temperature, annual 3-day heat wave magnitude, and the 81 percentile temperature (not shown) were similar to the results for the 97.5 percentile. All indicate that the RCM results are much more realistic than the respective driving GCMs in simulating the present climate and thus are considered also to be more credible for projecting future climate changes.

b. *Annual 3-day heat waves and number of heat wave days*

Maps of the average annual 3-day heat wave temperature changes in the 2090s for the high emissions scenarios (Figs. 2a,c) illustrate differences arising from the climate sensitivity of the driving CGCMs. Over most areas, the future temperature change is at least 3°C. Despite higher effective CO_2 concentrations, the temperature increases in the RCM-P are generally less than in the RCM-H. In the RCM-H, about 35% of the area has temperature increases in excess of 5°C and 6% of the area has increases above 8°C. In the RCM-P, the total percentage area above 5°C is only 8% and there are no grid points with values as high as 8°C. The changes are statistically significant (white areas indicate areas not statistically significant) over virtually the entire domain for both simulations. The magnitudes of the future changes are large compared to historical variations. The set of long-term stations was used to calculate the variability of average annual 3-day heat wave temperature for consecutive 10-yr blocks over the period of 1895–2008. The average standard deviation of this metric was 0.6°C, small compared to the future changes over most of the domain.

The regional patterns of future changes differ from the single PCM realization results of Meehl and Tebaldi (2004) for the business-as-usual scenario. They found maximum increases in the hottest 3-day period over

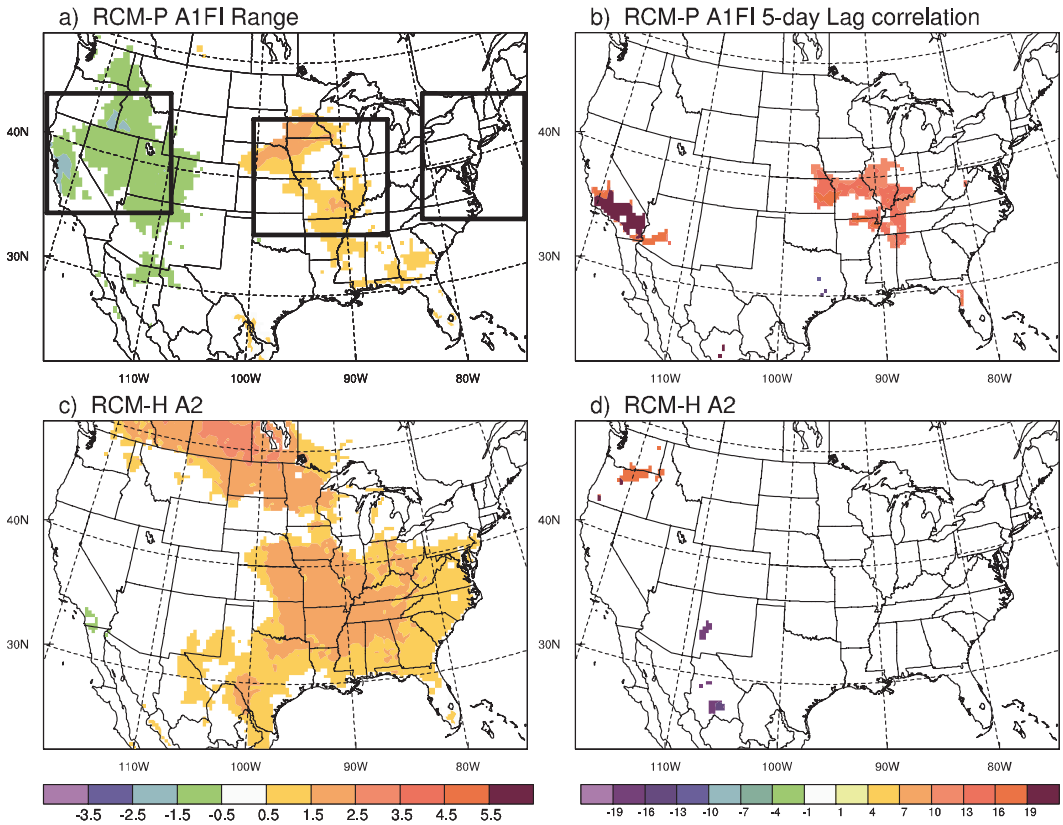

FIG. 3. Projections of the (a),(c) change in temperature range (°C) and (b),(d) 5-day lag autocorrelation coefficient (%). Simulations include the (a),(b) RCM-P A1Fi and (c),(d) RCM-H A2 emissions scenarios. Outlined in Fig. 3a are the three regions illustrated in Fig. 4.

the southern and western United States. Our RCM-P (A1Fi) projects maximum increases in the central United States, while the RCM-H (A2) produces large increases over almost the entire United States, maximized in the northwest United States Such contrast may arise from the different emissions scenario, different climate sensitivities, and/or the downscaling improvements. The suite of RCM simulations provides a range of future outcomes needed for assessing projection uncertainties.

The average number of days in heat waves in the 2090s (Figs. 2b,d) increases by 30–60 day yr^{-1} over much of the western United States in both the RCM-H and RCM-P simulations, while relatively smaller increases occur in the northeast quadrant of the United States. Considering that the average annual number of days in the present climate is typically 2–5 (not shown), these are substantial increases. The RCM-H (but not the RCM-P) also produces large increases along the Gulf Coast and in Florida. The results are statistically significant (at the $p = 0.05$ level; white areas indicate areas not statistically significant) over most of the domain, the only notable exceptions being southeast Texas in the RCM-P simulation.

c. *Range, autocorrelation, frequency, and spectra*

The changes in the number of heat wave days (Figs. 2b,d) utilize the same temperature threshold for both the control and the future simulations. However, a warmer overall climate will lead to a degree of acclimatization to the heat by the human population located in presently vulnerable areas (see later discussion related to Fig. 3). Other relevant measures of change are the variability and persistence of temperature. Several metrics were computed to examine this aspect of change. The variability was assessed by analyzing the difference in temperature between the 97.5 percentile and the mean temperatures, both calculated for the same simulation and referred to herein as the "temperature range." The persistence was measured by calculating the lag autocorrelation—in this case, using a 5-day lag. Both variability and persistence were examined in more detailed by calculating the variance spectrum using the fast Fourier transform.

The differences in the temperature range (difference between the 97.5 and 50th percentiles) between future simulations and control simulations (Figs. 3a,c) indicate that the changes are not statistically significant over large portions of the domain. There are statistically significant decreases in the range over portions of the western United States in the RCM-P simulation. Statistically significant increases in the range are found in small portions of the central United States in the RCM-P simulation and considerably larger area in the RCM-H simulation extending from south-central Canada southward through the central United States to the Gulf and southern Atlantic Coasts.

The changes in the 5-day lag autocorrelation (Figs. 3b,d) are not statistically significant over most of the domain. The only exceptions are increases in the correlation in the central United States and southern California in the RCM-P and a small area in the northwestern United States in the RCM-H.

The changes in the frequency of occurrence distribution (FOD) of daily temperature are illustrated in Fig. 4 for three areas suggested by Fig. 3a (and outlined in this figure) from the RCM-P A1Fi simulation: (i) the western United States, where the temperature range decreases; (ii) the central United States, where the temperature range increases; (iii) and the northeastern United States, where the temperature range changes are not statistically significant. Each FOD is an average of the individual FODs for all of the grid points within a particular box. In all cases, the shift in the FOD toward higher temperatures is large and only slightly smaller than the half-width of the FOD. For the central region, the high tail of the future FOD is extended, indicating that this model simulates more frequent occurrences of the warmest days with respect to its own climatology. For the western region, the future FOD is narrower, indicating a less extreme climate. There is relatively little difference between the present and future FOD widths for the Northeast. However, for all regions, the changes in the FOD shapes are small compared to the shifts in the temperature distribution toward warmer temperatures.

Changes in the variance spectra were computed for two period intervals—3–7 and 7–14 days—shown in Fig. 5. For the RCM-P A1Fi simulation, there are increases in variance over much of the central United States and southern Canada in the 3–7-day interval and decreases over portions of the western United States in the 7–14-day interval. The results for the RCM-H A2 simulation are not very consistent with RCM-P with increases over portions of the southeastern United States, Mexico, and southwestern United States in the 3–7-day interval; in the 7–14-day interval, there are decreases over the portions of the far western United States and increases over small portions of Mexico, southern Canada, and the southern United States. However, for most of the rest of the domain, the changes are not statistically significant.

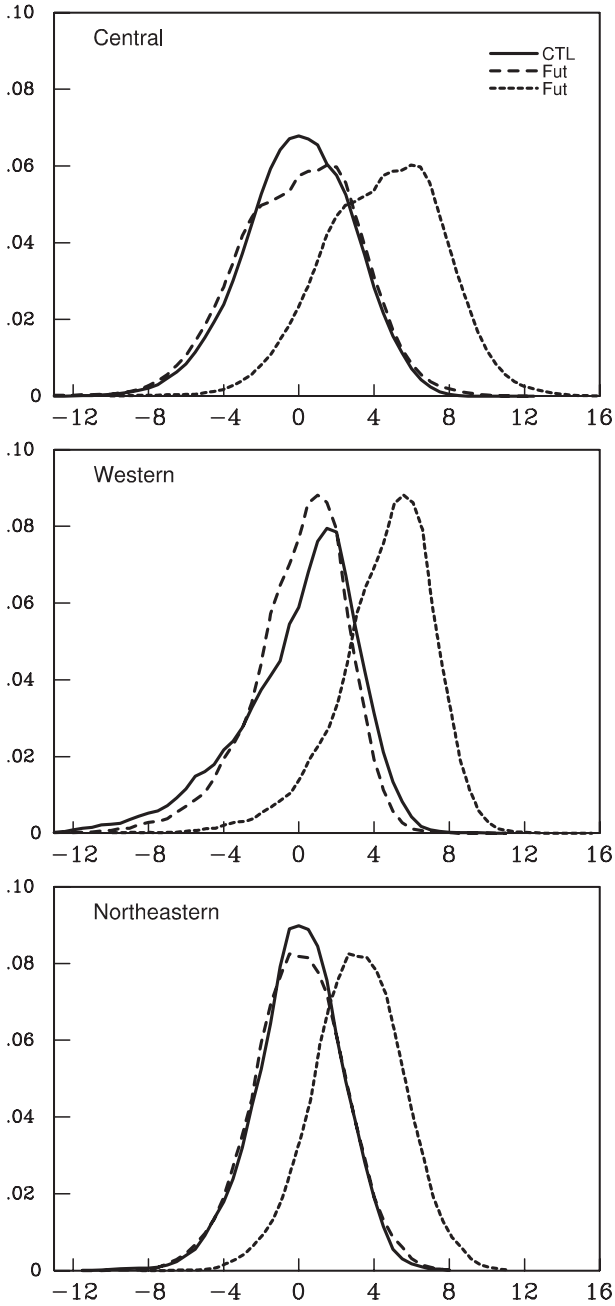

FIG. 4. FOD of daily temperature (expressed as deviations from the mean) for the three regions outlined in Fig. 3a for the RCM-P A1Fi simulation. The short-dashed line shows the future simulation FOD using the control simulation mean to calculate deviations, illustrating the climatology shift. The long-dashed line shows the future simulation FOD using the future simulation mean to calculate deviations, illustrating changes in the distribution shape.

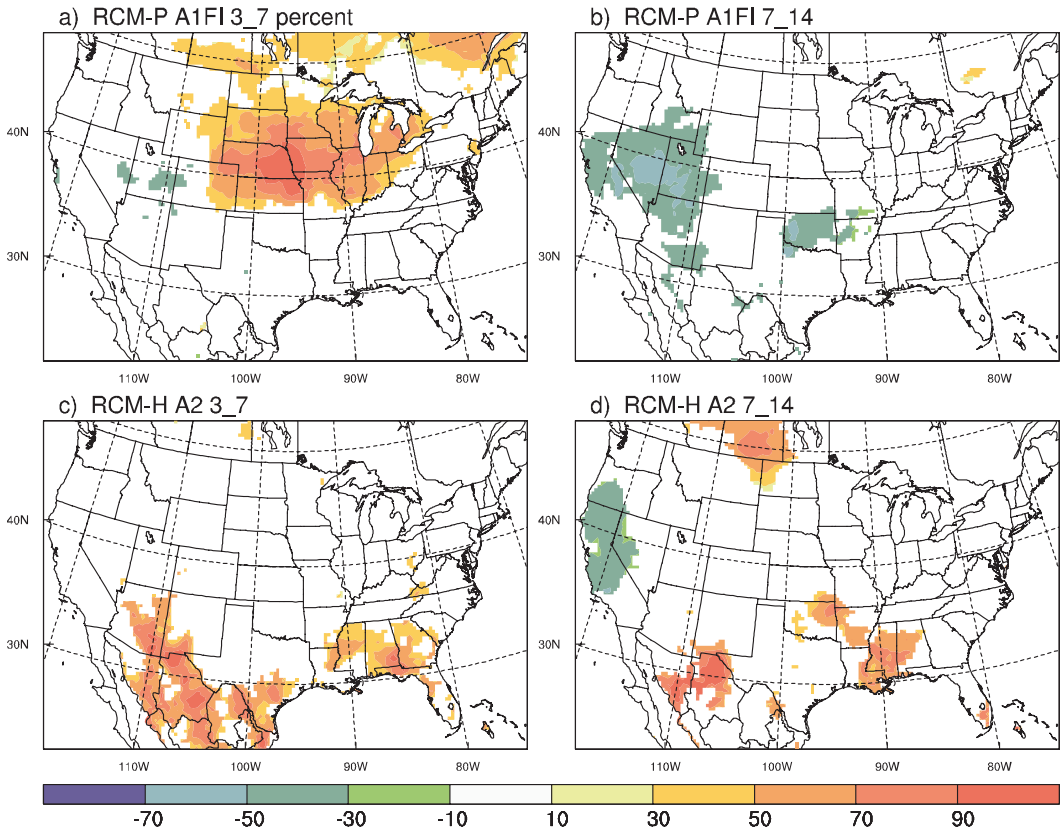

FIG. 5. Projections of variance spectra changes (%). Simulations include the (a),(b) RCM-P A1Fi and (c),(d) RCM-H A2 emissions scenarios. The variance is integrated for two bands of periods of days: (a),(c) 3–7 and (b),(d) 7–14. White areas indicate areas where changes are not statistically significant.

With respect to the heat wave results, the spectra integrate the variance for all days, not just heat wave days, and thus it is not necessary that the heat wave results in Figs. 2, 3 be related. However, there is some correspondence, in that some areas with reduced variance are areas with a reduced temperature range and vice versa. For example, for the RCM-P A1Fi simulation, much of the western United States exhibits reduced spectral variance, while the central United States is characterized by increased variance in the 3–7-day band. Since the temperature range results, shown in Fig. 3a, are for 3-day heat waves, that band might be expected to show some correspondence.

d. *Heat waves in select urban areas*

A summary of the annual 3-day heat wave results for Chicago and the Northeast urban areas (Figs. 6a,b) indicates that the RCM-P increases projected for both areas are quite small (~1°C) for the B1 scenario in the 2090s and significant only at $p = 0.10$. In contrast, for the RCM-P A1Fi and the RCM-H A2 and B2 simulations, the increases are sizeable (3°–5°C) for Chicago and slightly smaller for the Northeast (2°–4°C). The latter results are all significant at $p = 0.01$.

Biases of the present-day annual 3-day heat wave temperature (simulated minus observed) are less than 1°C. The internal variability of the present-day simulations was compared with observed variability using as a measure the difference (denoted as "spread") between the annual 3-day heat wave temperature and the mean summer temperature. The model spreads are slightly smaller than observed in both regions, by about 0.4°C for Chicago and a slightly larger 1°C for the Northeast. The future changes simulated in the various experiments are much larger than the biases, providing some confidence that such large simulated changes are robust.

For the number of heat wave days (Figs. 6c,d), the projected changes under the B1 scenario are statistically insignificant (around +2 or less) in the RCM-P simulation. The RCM-P A1Fi simulation increases the number of days by 17 for Chicago and by 25 for the Northeast, both significant at $p = 0.01$. The RCM-H projected increase of 15 days for Chicago for the A2 scenario is also

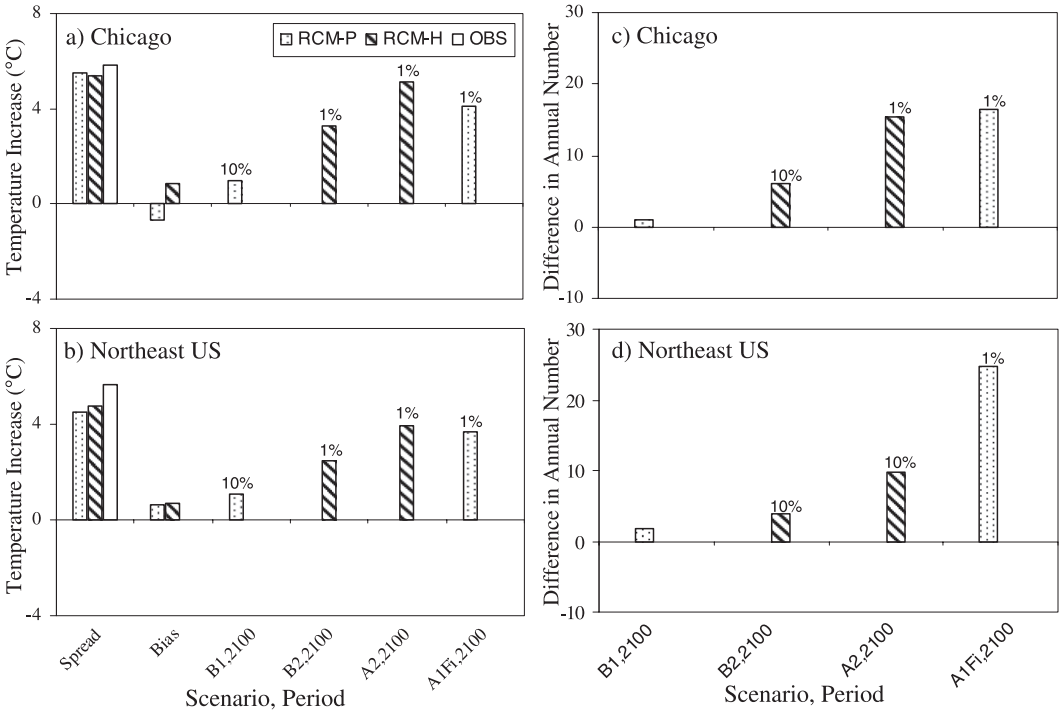

FIG. 6. Projections of (left) changes in the average annual 3-day heat wave temperature (°C) and (right) the annual average number of heat wave days for (a),(c) Chicago and (b),(d) the Northeast. The two sets of bars on the far left side of (a) and (c) compare the present-day annual 3-day heat wave temperature spread (from its own summer mean temperature as simulated and observed) and model biases (from observations). The simulations are arranged from left to right in order of increasing greenhouse gas concentrations. Percentages on top of the bars give the level of statistical significance.

significant at $p = 0.01$. The RCM-H A2 increase of 10 days for the Northeast and the increases of 6 and 4 days for Chicago and the Northeast, respectively, for the B2 scenario are significant at $p = 0.10$.

The annual heat waves were analyzed to determine changes in selected variables in addition to temperature in the areas of Chicago and the Northeast. For air quality, these were wind speed at 850 hPa and the depth of the planetary boundary layer (PBL). The two factors affect the dilution of harmful chemical species. For example, increasing wind speed increases the ventilation rate, while increasing PBL depth increases the mixing volume. For heat morbidity, specific humidity and surface wind speed were analyzed as additional factors. The changes in 850-hPa wind speed (Fig. 7) are mixed in sign and rather small in magnitude and are not statistically significant for any of the scenarios. The changes in surface wind speed (not shown) are similar. For Chicago, the PBL height exhibits a statistically significant change (at $p = 0.10$) only in the RCM-H A2 simulation (an increase of ~0.5 km). For the Northeast, the PBL height changes are not statistically significant. Specific humidity increases in all simulations for Chicago, but the changes are statistically significant (at $p = 0.01$) only for the RCM-P A1Fi simulation (increase of ~0.03 kg kg^{-1}). For the Northeast, the changes are statistically significant for RCM-H B2 ($p = 0.10$), RCM-H A2 ($p = 0.01$), and RCM-P A1Fi ($p = 0.01$).

The earlier-mentioned conditions were also analyzed for the larger number of heat wave days as defined by the control simulation thresholds and quantified in Fig. 2. The changes (not shown) in the wind, PBL height, and specific humidity conditions were not consistent among the simulations. For example, the RCM-P future simulations indicated lower wind speeds and specific humidity, while the RCM-H future simulations indicated higher winds speeds and specific humidity.

The representativeness of the results for Chicago and the Northeast were investigated by examining the temperature changes of the annual heat waves for 11 other urban areas (Fig. 8). The projected temperature changes are to first order similar among the entire set of urban areas. There is some tendency for the projected annual heat wave temperature increases to be smaller in urban areas near coasts (Los Angeles, San Francisco, Houston, Miami, the Northeast) compared to the inland locations.

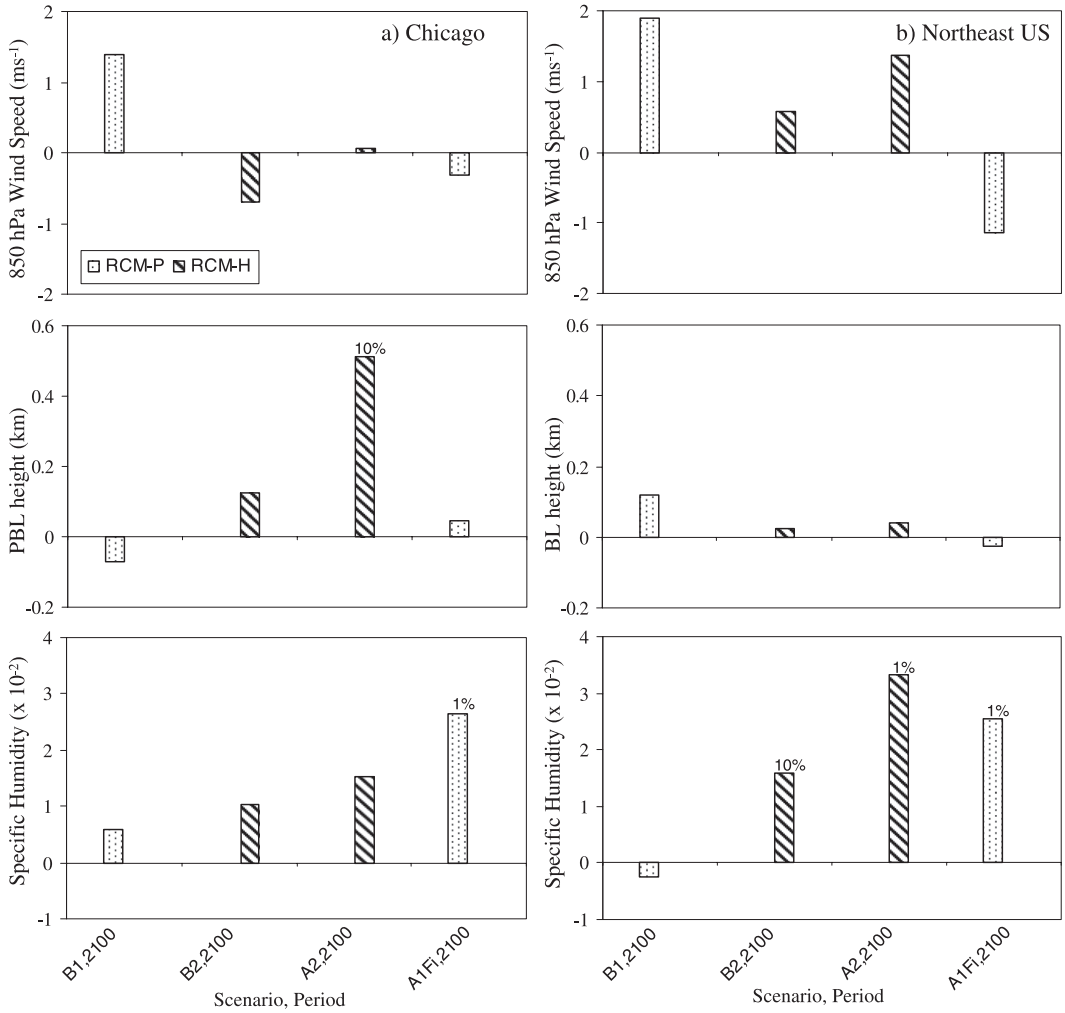

FIG. 7. Projections of changes in selected climate variables during the annual heat waves for (a) Chicago and (b) the Northeast. The simulations are arranged from left to right in order of increasing greenhouse gas concentrations. Variables included (top) wind speed at 850 hPa (m s^{-1}), (middle) PBL height (m), and (bottom) specific humidity (kg kg^{-1}).

4. Discussion

The superior simulation of the present-day regional climate by the RCM relative to the driving CGCMs provides the motivation for the application of the RCM to examine the potential for future changes in heat waves. The RCM simulations provide two key findings that address the purpose of this study. First, the projected changes in heat wave intensity and frequency are substantial by the 2090s for the higher (A1Fi, A2) and even moderately low (B2) emissions scenarios. However, the changes are quite small in the RCM-P simulation for the B1 scenario. Second, the RCM simulates substantially more intense and frequent heat wave conditions when driven by the HAD than by the PCM, inheriting the climate sensitivity of the driving CGCMs and indicating the extent to which the large-scale forcing affects local heat wave conditions. As a result, the changes for the annual heat waves in the 2090s projected by the RCM-H under the moderately high A2 emissions scenario are comparable to or greater than those projected by RCM-P under the very high A1Fi emissions scenario.

To illustrate the magnitude and potential significance of the projected changes, locations were identified where the historically observed (for the period 1991–2000) annual heat wave temperatures are similar to the projected values for the RCM-P and RCM-H simulations. For the following comparison, the values of the hottest of the annual heat waves are shown. For Chicago (hottest 3-day temperature = 32.3°C), the projected increase for the A2 (B2) scenario by the RCM-H of 7.7°C (3.9°C) leads to

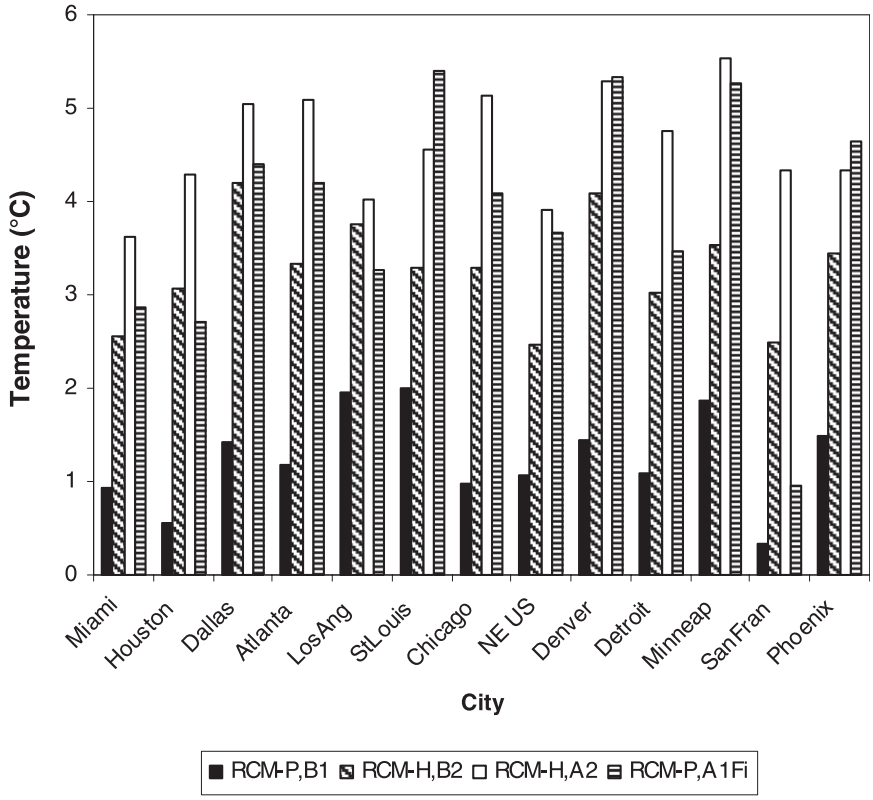

FIG. 8. Projections of changes in the average annual 3-day heat wave temperature (°C) for selected urban areas.

a projected value of 40.0°C (36.2°C), similar to the hottest 3-day temperature in Phoenix, Arizona (El Paso, Texas) for 1991–2000. The projected increase by the RCM-P of 5.7°C for the A1Fi scenario leads to a value of 38.0°C, which is comparable to present-day value of Tucson, Arizona. For New York City (hottest 3-day temperature = 32.4°C), the projected increase for the A2 (B2) scenario by the RCM-H of 3.9°C (1.7°C) leads to a projected value of 36.3°C (34.1°C), similar to that in El Paso (Columbia, South Carolina) in the present-day climate. The projected increase by the RCM-P of 2.5°C (5.5°C) for the A1Fi scenario leads to a value of 34.9°C, which is comparable to present-day values of Wichita Falls, Texas (Tucson). For both locations, the projected increases by the RCM-P for the B1 scenario are quite small.

These simulations do not indicate any potential exacerbating effects of adverse air quality, other than the direct influence of warmer temperature and higher humidity on chemical reactions, and perhaps even a mitigating effect. There were no significant changes in wind speed and PBL height in a majority of the simulations.

An examination of the entire suite of projections suggests that, under a high emissions path, there is a very high probability of a substantial increase in the frequency and intensity of heat waves by the end of the twenty-first century since such changes are produced by the RCM-P, a low climate-sensitivity model combination. There is the possibility that such large changes can be avoided under a low emissions scenario, as projected in the RCM-P B1 simulation. However, large increases still could occur in the moderately low emissions case, as projected in the RCM-H B2 simulation. Of course, more simulation experiments would provide a more complete suite of potential future outcomes. However, our judicious selection of experiments provides important insights into the possible ranges.

It is not possible to reliably estimate the potential effects of these climate outcomes. Over the course of the twenty-first century, considerable adaptation can occur. Indeed, recent changes, such as widespread adoption of air conditioning in northern areas, may already have reduced vulnerability (Davis et al. 2002), although the corresponding increase in emissions may result in even larger climate changes. The future changes in temperature range and overall variability are mixed, with some areas indicating increases and others decreases. In all cases such changes are small compared to the shift in the temperature distribution to warmer conditions, suggesting

the adaptation and acclimatization could reduce effects. Nevertheless, the elevated mortality during the 1995 and 1999 events illustrate that these areas remain vulnerable.

In comparison to the single CGCM results of Meehl and Tebaldi (2004), the RCM simulations illustrate that, although the RCM considerably reduces the biases of the CGCMs internal to the domain, there are considerable regional variations in future heat wave characteristics arising from the differences in the lateral boundary conditions from the driving CGCMs.

Acknowledgments. We thank the National Center for Atmospheric Research for the PCM data and David Hein, David Hassell, and Richard Jones for providing the HadAM3P data and for their technical assistance. We acknowledge the National Oceanic and Atmospheric Administration Forecast Systems Laboratory and the National Center for Supercomputing Applications at the University of Illinois at Urbana–Champaign for the supercomputing support. The research was partially supported by the U.S. Environmental Protection Agency Science to Achieve Results (STAR) Award EPA RD-83337301-0 and NOAA Contract EA133E-02-CN-0027. The views expressed are those of the authors and do not necessarily reflect those of the sponsoring agencies, the Desert Research Institute, or the Illinois State Water Survey.

REFERENCES

Changnon, S. A., K. E. Kunkel, and B. C. Reinke, 1996: Impacts and responses to the 1995 heat wave: A call to action. *Bull. Amer. Meteor. Soc.,* **77,** 1497–1506.

Christensen, J. H., T. R. Carter, and F. Giorgi, 2002: PRUDENCE employs new methods to assess European climate change. *Eos, Trans. Amer. Geophys. Union,* **83,** doi:10.1029/2002EO000094.

Davis, R. E., P. C. Knappenberger, W. M. Novicoff, and P. J. Michaels, 2002: Decadal changes in heat-related human mortality in the eastern United States. *Climate Res.,* **22,** 175–184.

Huth, R., J. Kysely, and L. Pokorna, 2000: A GCM simulation of heat waves, dry spells, and their relationships to circulation. *Climatic Change,* **46,** 29–60.

Johns, T. C., and Coauthors, 2003: Anthropogenic climate change for 1860 to 2100 simulated with the HadCM3 model under updated emissions scenarios. *Climate Dyn.,* **20,** 583–612, doi:10.1007/s00382-002-0296-y.

Kalkstein, L. S., 1993: Direct impacts in cities. *Lancet,* **342,** 1397–1399.

——, and J. S. Greene, 1997: An evaluation of climate/mortality relationships in larger U.S. cities and the possible impacts of a climate change. *Environ. Health Perspect.,* **105,** 84–93.

Kunkel, K. E., and X.-Z. Liang, 2005: GCM simulations of the climate in the central United States. *J. Climate,* **18,** 1016–1031.

Liang, X.-Z., L. Li, K. E. Kunkel, M. Ting, and J. X. L. Wang, 2004: Regional climate model simulation of U.S. precipitation during 1982–2002. Part I: Annual cycle. *J. Climate,* **17,** 3510–3529.

——, J. Pan, J. Zhu, K. E. Kunkel, J. X. L. Wang, and A. Dai, 2006: Regional climate model downscaling of the U.S. summer climate and future change. *J. Geophys. Res.,* **111,** D10108, doi:10.1029/2005JD006685.

——, K. E. Kunkel, G. A. Meehl, R. G. Jones, and J. X. L. Wang, 2008: Regional climate models downscaling analysis of general circulation models present climate biases propagation into future change projections. *Geophys. Res. Lett.,* **35,** L08709, doi:10.1029/2007GL032849.

Meehl, G., and C. Tebaldi, 2004: More intense, more frequent, and longer lasting heat waves in the 21st century. *Science,* **305,** 994–997.

Nakicenovic, N. J., and Coauthors, 2000: *Special Report on Emissions Scenarios*. Cambridge University Press, 599 pp.

Palecki, M. A., S. A. Changnon, and K. E. Kunkel, 2001: The nature and impacts of the July 1999 heat wave in the midwestern United States: Learning from the lessons of 1995. *Bull. Amer. Meteor. Soc.,* **82,** 1353–1367.

Pope, V. D., M. L. Gallani, P. R. Rowntree, and R. A. Stratton, 2000: The impact of new physical parametrizations in the Hadley Centre climate model: HadAM3. *Climate Dyn.,* **16,** 123–146.

Rowell, D. P., 2005: A scenario of European climate change for the late twenty-first century: Seasonal means and interannual variability. *Climate Dyn.,* **25,** 837–849.

Washington, W. M., and Coauthors, 2000: Parallel climate model (PCM) control and transient simulations. *Climate Dyn.,* **16,** 755–774.

Whitman, S., G. Good, E. R. Donoghue, N. Benbow, W. Shou, and S. Mou, 1997: Mortality in Chicago attributed to the July 1995 heat wave. *Amer. J. Public Health,* **87,** 1515–1518.